Monitoring galactolipid digestion and simultaneous changes in lipid-bile salt micellar organization by real-time NMR spectroscopy

Moulay Sahaka, Olivier Bornet, Achille Marchand, Dominique Lafont, Brigitte Gontero, Frédéric Carrière, Hélène Launay

▶ **To cite this version:**

Moulay Sahaka, Olivier Bornet, Achille Marchand, Dominique Lafont, Brigitte Gontero, et al.. Monitoring galactolipid digestion and simultaneous changes in lipid-bile salt micellar organization by real-time NMR spectroscopy. Chemistry and Physics of Lipids, 2024, 258, pp.105361. 10.1016/j.chemphyslip.2023.105361 . hal-04306594

HAL Id: hal-04306594
https://hal.science/hal-04306594

Submitted on 25 Nov 2023

HAL is a multi-disciplinary open access archive for the deposit and dissemination of scientific research documents, whether they are published or not. The documents may come from teaching and research institutions in France or abroad, or from public or private research centers.

L'archive ouverte pluridisciplinaire **HAL**, est destinée au dépôt et à la diffusion de documents scientifiques de niveau recherche, publiés ou non, émanant des établissements d'enseignement et de recherche français ou étrangers, des laboratoires publics ou privés.

Distributed under a Creative Commons Attribution - NonCommercial - NoDerivatives 4.0 International License

Preprint of Sahaka et al. *Chemistry and Physics of Lipids* (2024) 258:105361

https://doi.org/10.1016/j.chemphyslip.2023.105361

Monitoring galactolipid digestion and simultaneous changes in lipid-bile salt micellar organization by real-time NMR spectroscopy

Moulay Sahaka[a], Olivier Bornet[b], Achille Marchand[a], Dominique Lafont[c], Brigitte Gontero[a], Frédéric Carrière[a*] and Hélène Launay[a*]

[a] Aix Marseille Univ, CNRS, UMR7281 Bioénergétique et Ingénierie des Protéines, 31 Chemin Joseph Aiguier, 13009 Marseille, France.

[b] NMR Platform, Institut de Microbiologie de la Méditerranée, Aix Marseille Univ, 13009 Marseille, France

[c] Laboratoire de Chimie Organique 2-GLYCO, ICBMS UMR 5246, CNRS-Université Claude Bernard Lyon 1, Université de Lyon, bâtiment Lederer, 1 rue Victor Grignard, 69622 Villeurbanne Cedex, France

[*]Corresponding authors: carriere@imm.cnrs.fr and hlaunay@imm.cnrs.fr

Abstract

The use of Nuclear Magnetic Resonance spectroscopy for studying lipid digestion *in vitro* most often consists of quantifying lipolysis products after they have been extracted from the reaction medium using organic solvents. However, the current sensitivity level of NMR spectrometers makes possible to avoid the extraction step and continuously quantify the lipids directly in the reaction medium. We used real-time ^{1}H NMR spectroscopy and guinea pig pancreatic lipase-related protein 2 (GPLRP2) as biocatalyst to monitor *in situ* the lipolysis of monogalactosyl diacylglycerol (MGDG) in the form of mixed micelles with the bile salt sodium taurodeoxycholate (NaTDC). Residual substrate and lipolysis products (monogalactosyl monoacylglycerol (MGMG); monogalactosylglycerol (MGG) and octanoic acid (OA) were simultaneously quantified throughout the reaction thanks to specific proton resonances. Lipolysis was complete with the release of all MGDG fatty acids. These results were confirmed by thin layer chromatography (TLC) and densitometry after lipid extraction at different reaction times. Using diffusion-ordered NMR spectroscopy (DOSY), we could also estimate the diffusion coefficients of all the reaction compounds and deduce the hydrodynamic radius of the lipid aggregates in which they were present. It was shown that MGDG-NaTDC mixed micelles with an initial hydrodynamic radius r_H of 7.3 ± 0.5 nm were changed into smaller micelles of NaTDC-MGDG-MGMG of 2.3 ± 0.5 nm in the course of the lipolysis reaction, and finally into NaTDC-OA mixed micelles (r_H of 2.9 ± 0.5 nm) and water soluble MGG. These results provide a better understanding of the digestion of galactolipids by PLRP2, a process that leads to the complete micellar solubilisation of their fatty acids and renders their intestinal absorption possible.

Keywords: Enzyme, lipase, galactolipases, galactolipids, digestion, lipolysis, pancreatic lipase related protein 2, MGDG, NMR spectroscopy, DOSY, PGSE, thin layer chromatography.

Abbreviations: C8-MGDG, monogalactosyl-dioctanoyl glycerol; DOSY, diffusion-ordered spectroscopy; FA, fatty acid; FFA, free fatty acid; GPLRP2, guinea pig pancreatic lipase related protein 2; HDO, semiheavy water; MGDG, monogalactosyl-diacyl glycerol; MGG, monogalactosyl glycerol; MGMG, monogalactosyl-monoacyl glycerol; NaTDC; sodium taurodeoxycholate; OA, octanoic acid; pD, pH in D_2O; PLRP2, pancreatic lipase related protein 2; TLC, thin-layer chromatography; TES, N-tris[hydroxymethyl]methyl-2-aminoethane-sulfonic acid;

1. Introduction

The use of nuclear magnetic resonance (NMR) spectroscopy for studying lipid digestion *in vitro* usually consists in quantifying the residual substrate (triacylglycerol; TAG) and its lipolysis products (diacylglycerols, monoacylglycerols, and free fatty acids) after these compounds have been extracted from the reaction medium with organic solvents (Deng et al., 1990; Joyce et al., 2016; Juneja et al., 1989; Martin-Rubio et al., 2019; Nieva-Echevarria et al., 2017a, b, c, d; Nieva-Echevarria et al., 2016, 2017e, f; Nieva-Echevarría et al., 2014). Most of the time, the TAG substrate is dispersed as an oil-in-water emulsion with surfactants. Some studies have also been dedicated to the fate of the surfactants used to prepare these emulsions, such as the citric acid esters of mono- and diglycerides (CITREM) that can also be hydrolysed by digestive lipases (Amara et al., 2014). The supramolecular assembly of the lipid substrate and lipolysis products in large lipid droplets and micelles renders their quantification by spectroscopic methods such as liquid NMR not as straightforward as that of isolated molecules. Indeed, the tumbling of the large aggregates is significantly slower than that of the individual molecules and these slower motions induce larger signal widths (Furó, 2005). To avoid these caveats, lipid aggregates can be dissociated in organic solvents, what is achieved upon lipid extraction. Therefore, NMR is often used after extraction as other analytical methods like chromatography or mass spectrometry. While this approach allows a robust quantification from aliquots collected in the course of the lipolysis reaction, it does not allow, however, a continuous monitoring of the digestion. Moreover, lipid extraction is time consuming.

Nevertheless, the development of more sensitive NMR spectrometers resulted in short acquisition times (*ca* min per spectrum) compared to the time-course of the hydrolysis. As a consequence, it has already made it possible to monitor enzymatic reactions in real time (Her et al., 2015). “Real time NMR spectroscopy” or “Time-Resolved NMR spectroscopy” is a widely used tool for monitoring biocatalysed glycan hydrolysis or transfer (Eixelsberger et al.,

2012; Haas et al., 1992; Jin et al., 2020; Tyl et al., 2004). Real time NMR also enabled the *in-situ* monitoring of lipase-catalyzed reactions in organic solvents (deuterated chloroform or benzene) (Vallikivi et al., 2004; Waudby et al., 2013). In addition, a recent ^{1}H NMR study on the hydrolysis of a triglyceride emulsion by crustacean lipases has shown that lipolysis products could be quantified directly in an aqueous reaction media (D_2O/H_2O) (Timchenko et al., 2022). Using organic solvent for lipid extraction is therefore not necessary. As mentioned above, the organization of lipid substrates and lipolysis products in large supramolecular assemblies dispersed in aqueous media affects the NMR spectrum, but this occurs without compromising quantification, even using short acquisition times. All the conditions are therefore met to monitor the digestion of lipids in real-time with ^{1}H NMR spectroscopy without solvent extraction.

Besides, skipping the extraction step provide the great opportunity to also probe for the supramolecular organization *in-situ.* Liquid NMR spectroscopy is able to probe for the translational motions of the lipid aggregates that clusters the molecules. Pulsed Field Gradients (PFG) can be used to encode the position of the molecules that give rise to the ^{1}H resonance before a diffusion delay. The ^{1}H NMR spectrum is then acquired after reverse PFG (Stejskal and Tanner, 1965). This diffusion-ordered NMR spectroscopy (DOSY) method enables the ^{1}H resonances intensity to be modulated according to the translational diffusion of the molecules to which they belong. It is used to experimentally determine the size (hydrodynamic radius) of lipid aggregates by measuring their translational diffusion coefficients. This method has already been used to monitor lipid digestion *in vitro* (Awad et al., 2018; Patil et al., 2019; Pena and Hirasaki, 2003).

Here, we report the use of NMR spectroscopy to monitor the *in vitro* digestion of galactolipids by guinea pig pancreatic lipase-related protein type 2 (GPLRP2). The substrate used was a synthetic monogalactosyl dioctanoylglycerol (C8-MGDG) associated with bile salts in mixed

micelles. We used ^{1}H-^{13}C heteronuclear correlation experiments to assign the ^{1}H NMR frequencies to protons of C8-MGDG, bile salts and the hydrolysis products, monogalactosyl monooctanoylglycerol (MGMG), monogalactosylglycerol (MGG), and free octanoic acid. A series of rapid 1D ^{1}H spectra (min) was recorded immediately upon launching the hydrolysis reaction, and the ^{1}H signals integrals were used to probe the molecular concentration of C8-MGDG, MGMG, MGG and OA. Our quantification strategy enabled us to cope with the heterogeneous and large signal linewidths that originate from the supramolecular organisations, and it was validated using quantitative thin layer chromatography coupled to densitometry. Using DOSY-NMR, we recorded the translational diffusion coefficients associated to the same ^{1}H signals, such that we could determine the size of the aggregates formed by the reaction compounds at different stages of the reaction.

2. Materials and methods

2.1. Reagents

Monogalactosyl dioctanoyl-glycerol (C8-MGDG; M_w=506 g/mole) was synthetised as previously described (Amara et al., 2009; Lafont et al., 2006; Sias et al., 2004). Deuterium oxide (D_2O), Galactose, N-tris[hydroxymethyl]methyl-2-aminoethane-sulfonic acid (TES), Sodium taurodeoxycholate (NaTDC), Sulphuric acid and Thymol were purchased from Sigma-Aldrich (Saint-Quentin Fallavier, France). Calcium chloride ($CaCl_2$) and sodium chloride (NaCl) were obtained from Euromedex (Souffelweyersheim, France). Acetonitrile, chloroform, ethanol, and methanol were all HPLC grade from Carlo Erba (Peypin, France).

2.2. Production and purification of GPLRP2

Recombinant GPLRP2 was produced in *Aspergillus orizae* and purified as previously described (Hjorth et al., 1993). Aliquots of GPLRP2 were freeze-dried, suspended in the buffer solution prepared for the reactions in H_2O or D_2O, and finally incubated for 48 h at 4°C to reach H/D exchange equilibrium. The aliquots were then kept at -20°C until the reactions were performed. Before being added to the substrates, the aliquots were thawed and diluted to 1000 nM.

2.3. Preparation of C8-MGDG–NaTDC

To prepare C8-MGDG–NaTDC micelles, C8-MGDG was suspended in buffer solution containing 65.5 mM NaTDC, 500 mM TES buffer, 100 mM NaCl and 5 mM $CaCl_2$, in D_2O at pD 8 or H_2O at pH 8. The suspension was then heated to 65 °C for 5 min, vortexed and sonicated for 8 min to obtain micelles. C8-MGDG concentration was 50 mM and NaTDC to C8-MGDG molar ratio was 1.3.

2.4. Monitoring C8-MGDG hydrolysis by NMR spectroscopy

The lipolysis reaction was carried out by adding 50 µL of GPLRP2 solution (1000 nM) to 450 µL of C8-MGDG–NaTDC micelles to obtain 100 nM enzyme concentration. Both D_2O and H_2O solvent have been used in the present study, the advantage of working with D_2O being the easier solvent suppression efficiency by NMR. The suppression of the H_2O or residual HOD signal in ^1H 1D NMR spectra was achieved using highly selective presaturation at 4.7 ppm (recycling delay of 2s saturated with a power of 7.7 W). The galactose resonances that have frequencies close to that of water were better resolved with using the D_2O solvent so the deuterated solvent was preferred. In H_2O, only the glycerol or acyl chain resonances were well resolved, except the H2 glycerol resonance of MGG. Besides, the present reaction conditions in D_2O were identical to those of a previous study in which lipolysis was monitored by FTIR (Sahaka et al., 2023). Thus, NMR and FTIR analytical monitoring could be compared. The ^1H acquisition time was 340 ms, the spectral width 20 ppm, and 32 scans were accumulated for a total duration of 2 min per spectrum. One ^1H NMR spectrum was recorded before the addition of the enzyme. After enzyme addition, a series of 2-minutes spectra were recorded for 7 hours and a final spectrum was recorded after 16h 37min of incubation. All spectra were recorded at 37°C, on a Bruker Avance III 600 MHz spectrometer equipped with a TCI cryoprobe, using Topspin 3. software. Fourier transforms were performed with nmrPipe software (Delaglio et al., 1995), the data were then exported in text format and integrated into Spectra Manager V.2.07®.

The ^1H resonances were assigned to all compounds present in the reaction mixture using two dimensional ^1H-^{13}C heteronuclear correlation ^{13}C-^1H NOESY, TOCSY and HSQC spectra of bile salts alone and the reaction mixture before adding the enzymes (time 0) and upon completion hydrolysis (after more than 16 hours). To enable the assignment of the proton

resonances belonging to the intermediate MGMG product, a reaction was stopped after 20 min by incubation at 100°C for 10 min to denature the enzyme. ^{1}H-^{13}C heteronuclear experiments were recorded after the heat-denaturation step.

2.5. Quantification of substrate and products concentrations from ^{1}H NMR resonances

^{1}H NMR resonance signals that were sufficiently isolated were integrated at various times during the entire reaction. The values obtained were used to estimate the concentrations of the reaction compounds, using equation (1).

$$C_x(t) = \frac{A_x^{H_i}(t)}{Pc_x^{H_i}} \qquad (1)$$

With $C_x(t)$: Concentration of compound x, at time t

H_i: H protons of carbon i.

$A_x^{H_i}(t)$: Integral of H_i proton signal of compound x at time t

$Pc_x^{H_i}$: Proportionality coefficient relating $A_x^{H_i}$ to the concentration C_x.

The quantification using equation (1) requires knowing the values of the proportionality coefficients (Pc) for each compound x and proton H_i.

Since the concentrations of C8-MGDG before the reaction (t_0), MGG and free OA concentrations after the completion of the reaction (t_f) were known ($C_{MGDG}(t_0)$ = 50 mM, $C_{MGG}(t_f)$ = 50 mM, $C_{OA}(t_f)$ = 100 mM), the Pc of their protons were easily determined using equation (2), (3) and (4).

$$Pc_{MGDG}^{H_i} = \frac{A_{MGDG}^{H_i}(t_0)}{C_{MGDG}(t_0)} \quad (2)$$

$$Pc_{MGG}^{H_i} = \frac{A_{MGG}^{H_i}(t_f)}{C_{MGG}(t_f)} \qquad (3)$$

$$Pc_{OA}^{H_i} = \frac{A_{OA}^{H_i}(t_f)}{C_{OA}(t_f)} \qquad (4)$$

2.6. Characterization of galactolipid-bile salt micellar organization (aggregates size)

The supramolecular organizations formed by C8-MGDG, bile salts and lipolysis products before and during the lipolysis reaction were characterized using DOSY-NMR with bi-polar PFG stimulated echo experiments. Two pairs of bipolar square-shaped z-gradients of 2.8 ms (δ) were used to encode and decode the z-axis particle position, spaced with a delay (Δ) of 200 ms. A series of 10 spectra were recorded with gradient powers (G) ranging from 98% to 2% of the maximum gradient strength (0.5 $T.m^{-1}$) using a quadratic ramp. The spectra were transformed in Topspin 4.3 and nmrPipe (Delaglio et al., 1995), and the diffusion analysis was performed in Dynamic Center 2.8 and Octave (Eaton et al., 2016).

For each of these 10 spectra, the signal integral of the above-mentioned assigned ^1H resonances were quantified as function of gradient power (PFG -NMR). The spectra were transformed by nmrPipe (Delaglio et al., 1995) and exported into the Octave suite (Eaton et al., 2016). The diffusion coefficient (D, $m^2.s^{-1}$) was determined using the Stejskal–Tanner equation (5):

$$\ln\left(\frac{I_G}{I_0}\right) = D.\left[\Delta - \frac{\delta}{3}\right].(\delta.G.\gamma_H)^2 \qquad (5)$$

with I_G: Signal integral as a function of the gradient strength,

I_0: Integral in the absence of gradient,

γ_H: Proton gyromagnetic ratio (267.52 10^6 $rad.s^{-1}.T^{-1}$).The hydrodynamic radius (r_H) associated with a given diffusion coefficient was determined using the Stokes–Einstein equation (6):

$$r_H = \frac{k_B.T}{6\pi.D.\eta_{(T)}} \qquad (6)$$

with k_B : Boltzmann constant (1.38 10^{-23} $kg.m^2.s^{-2}.K^{-1}$),

T: Temperature in Kelvin,

$\eta_{(T)}$ (Viscosity) $= 2.41 \,.\, 10^{\frac{247.8}{T-140}-5}$ (kg.m^{-1}.s^{-1}).

2.7. Analysis of C8-MGDG lipolysis by TLC and densitometry

GPLRP2 was added to C8-MGDG–NaTDC micelles to obtain 100 nM enzyme concentration, in D_2O, at 37 °C. The reaction volume was 200 µL. Aliquots of 25 µL were collected at different reaction times (0, 10, 20, 50, 90 and 120 min) and immediately mixed with 1 mL of a stop solution containing 200 mM HCl and 150 mM NaCl. Substrates and reaction products in aliquots were extracted with chloroform-methanol (2:1 v/v) and analysed using TLC and densitometry, as previously described (Sahaka et al., 2021).

3. Results and Discussion

3.1. Identification of specific protons and their resonances for monitoring C8-MGDG disappearance and the generation of lipolysis products using NMR spectroscopy

Prior to monitoring the lipolysis reaction, we first performed ^{1}H-^{13}C heteronuclear experiments to perform the assignment of the proton resonances in the mixture buffer (TES) and bile salts (NaTDC), as well as in the mixture buffer (TES), bile salts (NaTDC) and C8-MGDG (Figure 1). The protons resonances of the TES and NaTDC were identical with or without the substrate (shown in Figure 1 without specific assignment). Proton resonances of lipolysis products (C8-MGMG, MGG and free OA) were assigned after recording ^{1}H-^{13}C heteronuclear spectra of the reaction mixture stopped after 20 min of hydrolysis and at completion of the reaction (Figure 2). The ^{1}H and ^{13}C chemical shifts of the reaction compounds, deduced from these spectra, are presented in Table 1. The resonances obtained for OA protons were similar to those in the database (Delaglio et al., 1995; Eaton et al., 2016).

3.2. Estimation of residual substrate and lipolysis products concentrations from ^{1}H NMR resonances

The evolution of the ^{1}H NMR spectrum of the C8-MGDG-NaTDC micelles solution in the presence of 100 nM GPLRP2 was recorded as a function of time (Figure 3). The intensity of proton resonances assigned to C8-MGDG (H2', H2, H6'') decreased quickly in favour of those of MGMG (H2', H2) and free OA (H2'). At the end of the reaction, only the resonances from MGG (H1'') and free OA proton were observed, indicating that the lipolysis was complete with the release of the two acyl chains initially bound to C8-MGDG. The glycerol H2 resonance of MGG has a frequency similar to that of water and is removed by the solvent suppression sequence.

Any resonance could be used for the quantification of the reaction compounds (C8-MGDG, MGMG, MGG, and free OA), but only those that were resolved enough to avoid overlaps with resonances from NaTDC and TES were used. The corresponding protons are indicated on the spectra in Figure 3. NMR signal integral is proportional to the number of protons and our quantification method enables to account for the differential linewidth caused by the differential supramolecular organisation. The quantification of each compound at various times t was performed using the integration of these resonance peaks ($A_x^{H_i}(t)$) and the equation (1) (see 2.5 Materials and Methods section), after estimating the values of the proportionality coefficients (Pc) for each compound x and proton H_i.

The proportionality coefficients (Pcs) for C8-MGDG, MGG and OA could be obtained from the initial concentration of C8-MGDG (50 mM) and final concentrations of MGG (50 mM) and OA (100 mM), respectively (Table 2). As expected, these Pcs are proportional to the number of identical protons within one molecule. However, they vary from one molecule to the other. One reason is the variation in the tumbling time of their corresponding molecules. The initial and final concentrations of the transient lipolysis product MGMG being zero, they could not be used to calculate the Pcs of MGMG (Pc_{MGMG}). However, the concentration of C8-MGMG during the reaction could be deduced from those of C8-MGDG and MGG, using the stoichiometry equation (7):

$$C_{MGMG}(t) = C_{MGDG}(t_0) - \left(C_{MGDG}(t) + C_{MGG}(t)\right) \qquad (7)$$

The MGMG concentrations obtained in this way were used to estimate the values of Pc_{MGMG} for protons H2' et H2 at all reaction times (Figure 4). These values (on average 3.10^{-5} mM^{-1} and $6{,}5.10^{-5}$ mM^{-1}, respectively) could be considered as constant throughout the reaction, with variation coefficients of 3 % for the protons of acyl chain carbon 2' ($Pc_{MGMG}^{H_{2'}}$) and 4 % for the

protons of glycerol carbon 2 ($Pc_{MGMG}^{H_2}$). The C8-MGMG concentrations were then calculated using the average values of these Pcs and the equation (1).

Among the resonance used for quantification, those belonging to the same compound, either H1a, H1b, H2 orH2' for C8-MGDG and H2 orH2' for MGMG, resulted in the same concentration and gave superimposed kinetic curves, thus confirming their assignment and the quantification procedure (Figure 5).

The time-course evolution of the concentrations of all compounds (Figure 6A), shows that C8-MGDG disappeared almost completely after 30 min of incubation. The disappearance of C8-MGDG correlates perfectly with the appearance of MGMG, MGG and free OA. As a validation, the total mass of the reaction compounds was found to be conserved throughout the reaction (Figure 7) with a coefficient of variation of about 1%. This further validates the quantification procedure and indicates that all products have been identified and quantified.

3.3. Validation of the NMR quantification procedure using TLC and densitometry

To validate the above quantification of substrate and products using ^{1}H NMR spectroscopy, we performed the same reaction with lipid extraction at various times and analysis using TLC-densitometry and thymol-sulfuric acid derivatization of galactosylated compounds. C8-MGDG, MGMG and MGG were revealed and quantified thanks to the galactose they contain after performing separate migrations for C8-MGDG and MGMG present in the organic phase and MGG present in the aqueous phase (Sahaka et al., 2021). Free OA concentrations were then estimated from C8-MGMG and MGG concentrations, using equation (8).

$$[Free\ OA] = [MGMG] + 2.[MGG] \qquad (8)$$

The concentrations and variation kinetics obtained (Figure 6B) were identical with those obtained by NMR spectroscopy (Figure 6A). In both cases, we could estimate the specific activity of GPLRP2 on C8-MGDG from the amount (µmoles) of OA released during the first 10 min of the reaction. The value obtained from NMR spectroscopy data was 903 U/mg, while a similar specific activity of 981 ± 97 U/mg was deduced from TLC analysis, with 1 U = 1 µmole of fatty acid released per min. These activities are in the same range as the specific activity (727 ± 67 U/mg) previously deduced from FTIR spectroscopy analysis of the same reaction (Sahaka et al., 2023).

As previously reported (Sahaka et al., 2023), it is worth noticing that 2 to 3-fold slower reaction rates are observed in D_2O than in H_2O. This could result from different experimental set-up, with for instance a slower mixing in the NMR tube compared to experiments performed under continuous mechanical stirring. However, a reduced activity of GPLRP2 was also observed in the course of dipalmitoylphosphatidylcholine (DPPC) hydrolysis in D_2O compared to H_2O (Mateos-Diaz et al., 2018). We assume that it is due in part to the lower dissociation and nucleophilicity of D_2O compared to H_2O. Indeed, the enzymatic hydrolysis of an ester bond in acylglycerols by lipases involves the formation of an acyl-enzyme intermediate that further reacts with a water molecule to release the free fatty acid (Carrière et al., 1997). Besides, a hydrogen bond with deuterium is slightly stronger than one with hydrogen and this can also impact the hydrogen bond network that stabilizes the tertiary structure of the enzyme (Cioni and Strambini, 2002; Katz, 1960; Katz and Crespi, 1966). It is thus possible that the interactions of MGDG and reaction intermediates with GPLRP2 active site are modified in D_2O compared to H_2O and this could result in lower reaction rates. Finally, it has also been shown that heavy water can impact the thermodynamic properties of lipid assemblies like the phase transition in phospholipid bilayers (Matsuki et al., 2005). We cannot exclude that the organisation of

MGDG-NaTDC micelles is different in D_2O compared to water and this may have an effect on their interaction with GPLRP2.

3.4. Analysis of the micellar organization of substrate and products using diffusion-ordered NMR spectroscopy

The diffusion coefficients (D) of NaTDC, C8-MGDG and reaction products (C8-MGMG, MGG and OA) were estimated in the reaction medium using the DOSY method (Figure 8 and Table 3). From these coefficients, the hydrodynamic radii (r_H) of the aggregates formed by these compounds were deduced using the Stokes-Einstein law as described in Material and method section (see 2.6 and Table 3).

The diffusion coefficient associated to the TES resonances (3.45 and 3.9 ppm) was 6×10^{-10} $m^2.s^{-1}$, indicated that the buffer molecules are free in solution, as expected.

The size of pure NaTDC aggregates as well as that of mixed NaTDC-fatty acid aggregates were estimated using the NaTDC methyl proton peaks at 0.9 and another resonance at 1.2 ppm (Figure 8A, B, C, D and E). When NaTDC was alone in the buffer solution, it formed aggregates with a r_H of 2.3 ± 0.2 nm. This size for NaTDC micelles is consistent with previous studies (Mazer et al., 1980). NMR studies have shown that NaTDC at high supramicellar concentration preferentially forms nonamers in equilibrium with dimers (Funasaki et al., 2006). According to Small et al, bile salts would first form dimers through hydrophobic interactions of their convex faces and then secondary larger micelles formed by hydrogen bonds (Small et al., 1969).

In the presence of C8-MGDG, the r_H estimated from NaTDC resonances increased to 7.3 ± 0.5 nm. The same hydrodynamic properties were probed by C8-MGDG glycerol H2 and acyl chain H2’ resonances, indicating that NaTDC formed mixed micelles with C8-MGDG (Figure 8B, E

and F and Table 3). This radius is close to that of C8-MGDG-NaTDC micelles previously measured by dynamic light scattering ($r_H \approx 5$ nm) (Belhaj et al., 2018). This is also close to NaTDC – lecithins mixed micelles at a molar ratio of 1.2 that have a r_H of 8.4 nm at 20-40°C in the presence of 150 mM NaCl (Mazer et al., 1980). Here, we worked with a NaTDC to C8-MGDG molar ratio of 1.3, in the presence of 100 mM NaCl, at 37°C. One can therefore assume that mixed bile salts-galactolipids micelles self-organize in an aqueous environment like mixed bile salts-phospholipid micelles and can be schematically represented as Mazer's disk-shaped micelles as depicted in Figure 9. We have previously shown that this molar ratio of 1.3 allows measuring the optimum activity of both human and guinea pig PLRP2s on C8-MGDG as substrate, as well as on natural long chain MGDG (Amara et al., 2010; Amara et al., 2009). It probably results in a micellar structure that is preferentially recognized by PLRP2.

After 20 min of reaction, when the C8-MGDG was partially hydrolyzed and the C8-MGMG intermediate product was close to its maximum concentration, the radius of the aggregates containing NaTDC decreased to about 2.3 ± 0.3 nm (Table 3). The same hydrodynamic properties were measured on the glycerol H2 and acyl H2' resonance of the remaining MGDG that has not been completely hydrolyzed yet. This indicates that the NaTDC-MGDG mixed micelles are reorganized in the course of the reaction, probably due to the presence of OA and MGMG molecules. The hydrodynamic properties inferred from C8-MGMG glycerol H2 and acyl chain H2' resonances are slightly smaller than those observed on NaTDC and MGDG protons (r_H 2 ± 0.5 nm), but the difference between the experimental diffusion coefficient determined for the NaTDC, MGDG and MGMG molecules is not significant (Figure 8E and F and Table 3, Figure 9). Also, the hydrodynamic properties of OA molecules cannot fit to equation (5) with a single coefficient diffusion (Figure 8 G), which indicates that OA assembles in several aggregates of various size and molecular composition. A binomial fit indicates that a large proportion of OA molecules are present in micelles of 2.2 ± 0.4 nm in size. Altogether,

we can infer that NaTDC, C8-MGDG, C8-MGMG and OA can assemble in mixed micelles that are smaller and less homogeneous in size than the initial NaTDC-C8-MGDG micelles. Another fraction of OA has a high diffusion coefficient of 4.5 10^{-10} $m^2.s^{-1}$, that may correspond to small aggregates (r_H 0.7 ± 0.1 nm) of few OA molecules. The relative quantification of the mixed-micelles or free OA is challenging to determine from their relative signal intensities because the latter also varies with the tumbling time of the molecules.

At the end of the reaction, when MGMG had also disappeared and products consisted in MGG and free OA, the radius of the aggregates containing NaTDC was 2.9 nm. Again, the DOSY data associated with the OA H2' resonances could not be fitted to equation (5) with a single diffusion coefficient, and a binomial fit indicated that a small proportion of OA molecules has the same diffusion coefficient estimated from the NaTDC protons (1.1 ± 0.2 10^{-10} $m^2.s^{-1}$), indicating that some OA is present in mixed micelles with NaTDC of 2.9 ± 0.5 nm (Figure 8C, D and G). The DOSY data recorded from the same OA H2' resonances at low gradient strength indicate the existence of particles with a smaller size. Using dynamic light scattering, Salentinig et al. have previously reported a similar r_H of 2.5 nm for NaTDC-OA mixed micelles at pH 7.1 and 25°C (Salentinig et al., 2014). Since OA (pK_a=6.5) is mostly ionized at the pH of the reaction (pD 8) and the final OA concentration of 100 mM being much above the critical micellar concentration of octanoate (CMC=13 mM;(Hayes and Gulari, 1994)), one can assume that octanoate micelles could also be formed (Figure 9). The size of these micelles of about 15 to 23 monomers has been estimated from previous neutron scattering data (1.17 ± 0.03 nm; (Hayden and Ma, 1992; Hayden et al., 1991)) and molecular dynamics simulations (1.27 nm; (Watanabe et al., 1988)). The size measured in our study is therefore higher and it suggests that OA remains associated in mixed micelles with NaTDC. The formation of water-soluble MGG at the end of the reaction was confirmed by the high diffusion coefficient of 9×10^{-10} $m^2.s^{-1}$

measured on its galactose H2' resonances, indicating that it was in the free molecule state (Figure 8D and F).

4. Conclusion

The enzymatic hydrolysis of a galactolipid (C8-MGDG) present in mixed micelles with bile salts was monitored in real time by recording H^1 NMR spectra of the reaction mixture. Integration of the proton peaks allowed the simultaneous estimation of residual C8-MGDG and lipolysis products (MGMG, MGG and OA) concentrations throughout the reaction. The hydrolysis was complete, confirming that the fatty acids at both *sn*-1 and *sn*-2 position of MGDG were released by the PLRP2 enzyme. The kinetics recorded by NMR spectroscopy were similar to those estimated by TLC analysis after lipid extraction and *in situ* transmission FTIR spectroscopy (Sahaka et al., 2023). Compared to this previous real time method, NMR spectroscopy allowed identifying and quantifying all lipolysis products including the water-soluble MGG. Another step forward was the simultaneously determination of the diffusion coefficients of these products, substrate and bile salts by DOSY. It allowed estimating the sizes of the micellar aggregates in which the substrate (C8-MGDG) was initially present mixed with bile salts and of the smaller micelles containing also the lipolysis products (MGMG, and OA) formed in the course of the lipolysis reaction. These results provide a better understanding of the digestion of galactolipids by PLRP2, a process that leads to the complete micellar solubilisation of their fatty acids and renders their intestinal absorption possible.

The above study opens the way to *in-situ* monitoring of lipid hydrolysis from the chemical and physico-chemical point of view. Skipping the extraction step speeds up and simplifies the experimental set-up, avoids the use of solvent, and opens the perspective of monitoring on-line processes using a non-invasive approach. For instance, NMR can be used to monitor lipid

accumulation in living microalgae (Bouillaud et al., 2019). The use of DOSY-NMR to characterise changes in the supramolecular assembly of lipids in the course of digestion also opens new perspective beside monitoring lipid hydrolysis. Changes in the size of TAG droplets, a critical parameter for the activity of lipases, could also be monitored in-situ thanks to PFG-DOSY in a restricted diffusion mode as demonstrated with lipid droplets accumulated in living algae (Gromova et al., 2015).

Declaration of competing interest

The authors declare that there are no conflicts of interest.

Author contribution

Moulay Sahaka was involved in the conception and design of the study, in acquisition, analysis and interpretation of data, in drafting the article and revising it critically for important intellectual content. Olivier Bornet was involved in acquisition, analysis and interpretation of NMR data, and revising the article critically for important intellectual content. Achille Marchand was involved in analysis and interpretation of NMR data. Dominique Lafont was involved in the chemical synthesis of C8-MGDG. Brigitte Gontero, was involved in revising the article critically for important intellectual content. Frédéric Carrière and Hélène Launay were involved in the conception and design of the study, in analysis and interpretation of data, in drafting the article and revising it critically for important intellectual content. All authors were involved in the final approval of the version to be submitted.

Funding

This work received the financial support of Agence Nationale de la Recherche (France) in the framework of the GALACTOLIPASE project (ANR-09-CP2D-06-01) and of the PhotOxIN project (ANR-22-CE44-0031-01), as well as the FEBS Excellence Award 2021.

Acknowledgements

The PhD thesis of Moulay Sahaka was supported by a fellowship from Aix Marseille Université, France. We are grateful to Dr Mohamed Vall Sidi Boune (Nouakchott University, Mauritania) for his critical review of chemical shift attributions.

References

Amara, S., Barouh, N., Lecomte, J., Lafont, D., Robert, S., Villeneuve, P., De Caro, A., Carriere, F., 2010. Lipolysis of natural long chain and synthetic medium chain galactolipids by pancreatic lipase-related protein 2. Biochim Biophys Acta 1801, 508-516.

Amara, S., Lafont, D., Fiorentino, B., Boullanger, P., Carriere, F., De Caro, A., 2009. Continuous measurement of galactolipid hydrolysis by pancreatic lipolytic enzymes using the pH-stat technique and a medium chain monogalactosyl diglyceride as substrate. Biochim Biophys Acta 1791, 983-990.

Amara, S., Patin, A., Giuffrida, F., Wooster, T.J., Thakkar, S.K., Bénarouche, A., Poncin, I., Robert, S., Point, V., Molinari, S., Gaussier, H., Diomande, S., Destaillats, F., Cruz-Hernandez, C., Carrière, F., 2014. *In vitro* digestion of citric acid esters of mono- and diglycerides (CITREM) and CITREM-containing infant formula/emulsions. Food & Function 5, 1409-1421.

Awad, T.S., Asker, D., Romsted, L.S., 2018. Evidence of coexisting microemulsion droplets in oil-in-water emulsions revealed by 2D DOSY (1)H NMR. J Colloid Interface Sci 514, 83-92.

Belhaj, I., Amara, S., Parsiegla, G., Sutto-Ortiz, P., Sahaka, M., Belghith, H., Rousset, A., Lafont, D., Carriere, F., 2018. Galactolipase activity of Talaromyces thermophilus lipase on galactolipid micelles, monomolecular films and UV-absorbing surface-coated substrate. Biochim Biophys Acta Mol Cell Biol Lipids 1863, 1006-1015.

Bouillaud, D., Farjon, J., Goncalves, O., Giraudeau, P., 2019. Benchtop NMR for the monitoring of bioprocesses. Magn Reson Chem 57, 794-804.

Carrière, F., Bezzine, S., Verger, R., 1997. Molecular evolution of the pancreatic lipase and two related enzymes towards different substrate selectivities. Journal of Molecular Catalysis B: Enzymatic 3, 55-64.

Cioni, P., Strambini, G.B., 2002. Effect of heavy water on protein flexibility. Biophys J 82, 3246-3253.

Delaglio, F., Grzesiek, S., Vuister, G.W., Zhu, G., Pfeifer, J., Bax, A., 1995. NMRPipe: a multidimensional spectral processing system based on UNIX pipes. J Biomol NMR 6, 277-293.

Deng, T., Noel, J.P., Tsai, M.D., 1990. A novel expression vector for high-level synthesis and secretion of foreign proteins in Escherichia coli: overproduction of bovine pancreatic phospholipase A2. Gene 93, 229-234.

Eaton, J., Bateman, D., Hauberg, S., Wehbring, R., 2016. GNU Octave A high-level interactive language for numerical computations, Octave version 4.2.1 ed.

Eixelsberger, T., Brecker, L., Nidetzky, B., 2012. Catalytic mechanism of human UDP-glucose 6-dehydrogenase: in situ proton NMR studies reveal that the C-5 hydrogen of UDP-glucose is not exchanged with bulk water during the enzymatic reaction. Carbohydr Res 356, 209-214.

Funasaki, N., Fukuba, M., Hattori, T., Ishikawa, S., Okuno, T., Hirota, S., 2006. Micelle formation of bile salts and zwitterionic derivative as studied by two-dimensional NMR spectroscopy. Chem Phys Lipids 142, 43-57.

Furó, I., 2005. NMR spectroscopy of micelles and related systems. Journal of Molecular Liquids 117, 117-137.

Gromova, M., Guillermo, A., Bayle, P.A., Bardet, M., 2015. In vivo measurement of the size of oil bodies in plant seeds using a simple and robust pulsed field gradient NMR method. Eur Biophys J 44, 121-129.

Haas, M.J., Cichowicz, D.J., Bailey, D.G., 1992. Purification and characterization of an extracellular lipase from the fungus Rhizopus delemar. Lipids 27, 571-576.

Hayden, M.R., Ma, Y., 1992. Molecular genetics of human lipoprotein lipase deficiency. Mol. Cell. Biochem. 113, 171-176.

Hayden, M.R., Ma, Y., Brunzell, J., Henderson, H.E., 1991. Genetic variants affecting human lipoprotein and hepatic lipases. Curr. Opin. Lipidol. 2, 104-109.

Hayes, D.G., Gulari, E., 1994. Improvement of enzyme activity and stability for reverse micellar-encapsulated lipases in the presence of short-chain and polar alcohols. Biocatalysis 11, 223-231.

Her, C., Alonzo, A.P., Vang, J.Y., Torres, E., Krishnan, V.V., 2015. Real-Time Enzyme Kinetics by Quantitative NMR Spectroscopy and Determination of the Michaelis−Menten Constant Using the LambertW Function. Journal of Chemical Education 92, 1943−1948.

Hjorth, A., Carrière, F., Cudrey, C., Wöldike, H., Boel, E., Lawson, D.M., Ferrato, F., Cambillau, C., Dodson, G.G., Thim, L., Verger, R., 1993. A structural domain (the lid) found in pancreatic lipases is absent in the guinea pig (phospho)lipase. Biochemistry 32, 4702-4707.

Jin, J.M., Bai, P., He, W., Wu, F., Liu, X.F., Han, D.M., Liu, S., Yang, J.K., 2020. Gender Differences in Patients With COVID-19: Focus on Severity and Mortality. Front Public Health 8, 152.

Joyce, P., Barnes, T.J., Boyd, B.J., Prestidge, C.A., 2016. Porous nanostructure controls kinetics, disposition and self-assembly structure of lipid digestion products. RSC Advances 6, 78385–78395.

Juneja, L.R., Yamane, T., Shimizu, S., 1989. Enzymatic method of inceasing phosphatidylcholine content of lecithin. J. Am. Oil Chem. Soc. 66, 714-717.

Katz, J.J., 1960. Chemical and Biological Studies with Deuterium. American Scientist 48, 544-580.

Katz, J.J., Crespi, H.L., 1966. Deuterated organisms: cultivation and uses. Science 151, 1187-1194.

Lafont, D., Carriere, F., Ferrato, F., Boullanger, P., 2006. Syntheses of an alpha-D-Gal-(1-->6)-beta-D-Gal diglyceride, as lipase substrate. Carbohydr Res 341, 695-704.

Martin-Rubio, A.S., Sopelana, P., Guillen, M.D., 2019. The key role of ovalbumin in lipid bioaccessibility and oxidation product profile during the in vitro digestion of slightly oxidized soybean oil. Food Funct 10, 4440-4451.

Mateos-Diaz, E., Sutto-Ortiz, P., Sahaka, M., Rodriguez, J.A., Carriere, F., 2018. IR spectroscopy analysis of pancreatic lipase-related protein 2 interaction with phospholipids: 3. Monitoring DPPC lipolysis in mixed micelles. Chem Phys Lipids 211, 77-85.

Matsuki, H., Okuno, H., Sakano, F., Kusube, M., Kaneshina, S., 2005. Effect of deuterium oxide on the thermodynamic quantities associated with phase transitions of phosphatidylcholine bilayer membranes. Biochim Biophys Acta 1712, 92-100.

Mazer, N.A., Benedek, G.B., Carey, M.C., 1980. Quasielastic light-scattering studies of aqueous biliary lipid systems. Mixed micelle formation in bile salt-lecithin solutions. Biochemistry 19, 601-615.

Nieva-Echevarria, B., Goicoechea, E., Guillen, M.D., 2017a. Behaviour of non-oxidized and oxidized flaxseed oils, as models of omega-3 rich lipids, during in vitro digestion. Occurrence of epoxidation reactions. Food Res Int 97, 104-115.

Nieva-Echevarria, B., Goicoechea, E., Guillen, M.D., 2017b. Effect of liquid smoking on lipid hydrolysis and oxidation reactions during in vitro gastrointestinal digestion of European sea bass. Food Res Int 97, 51-61.

Nieva-Echevarria, B., Goicoechea, E., Guillen, M.D., 2017c. Effect of the presence of protein on lipolysis and lipid oxidation occurring during in vitro digestion of highly unsaturated oils. Food Chem 235, 21-33.

Nieva-Echevarria, B., Goicoechea, E., Guillen, M.D., 2017d. Polyunsaturated lipids and vitamin A oxidation during cod liver oil in vitro gastrointestinal digestion. Antioxidant effect of added BHT. Food Chem 232, 733-743.

Nieva-Echevarria, B., Goicoechea, E., Manzanos, M.J., Guillen, M.D., 2016. A study by (1)H NMR on the influence of some factors affecting lipid in vitro digestion. Food Chem 211, 17-26.

Nieva-Echevarria, B., Goicoechea, E., Manzanos, M.J., Guillen, M.D., 2017e. (1)H NMR and SPME-GC/MS study of hydrolysis, oxidation and other reactions occurring during in vitro digestion of non-oxidized and oxidized sunflower oil. Formation of hydroxy-octadecadienoates. Food Res Int 91, 171-182.

Nieva-Echevarria, B., Goicoechea, E., Manzanos, M.J., Guillen, M.D., 2017f. Fish in Vitro Digestion: Influence of Fish Salting on the Extent of Lipolysis, Oxidation, and Other Reactions. J Agric Food Chem 65, 879-891.

Nieva-Echevarría, B., Goicoechea, E., Manzanos, M.J., Guillén, M.D., 2014. A method based on 1H NMR spectral data useful to evaluate the hydrolysis level in complex lipid mixtures. Food Research International 66, 379-387.

Patil, S.M., Li, V., Peng, J., Kozak, D., Xu, J., Cai, B., Keire, D.A., Chen, K., 2019. A Simple and Noninvasive DOSY NMR Method for Droplet Size Measurement of Intact Oil-In-Water Emulsion Drug Products. J Pharm Sci 108, 815-820.

Pena, A.A., Hirasaki, G.J., 2003. Enhanced characterization of oilfield emulsions via NMR diffusion and transverse relaxation experiments. Adv Colloid Interface Sci 105, 103-150.

Saele, O., Nordgreen, A., Olsvik, P.A., Hamre, K., 2010. Characterization and expression of digestive neutral lipases during ontogeny of Atlantic cod (Gadus morhua). Comp Biochem Physiol A Mol Integr Physiol 157, 252-259.

Sahaka, M., Amara, S., Lecomte, J., Rodier, J.D., Lafont, D., Villeneuve, P., Gontero, B., Carriere, F., 2021. Quantitative monitoring of galactolipid hydrolysis by pancreatic lipase-related protein 2 using thin layer chromatography and thymol-sulfuric acid derivatization. J Chromatogr B Analyt Technol Biomed Life Sci 1173, 122674.

Sahaka, M., Mateos-Diaz, E., Amara, S., Wattanakul, J., Gray, D., Lafont, D., Gontero, B., Launay, H., Carriere, F., 2023. In situ monitoring of galactolipid digestion by infrared spectroscopy in both model micelles and spinach chloroplasts. Chem Phys Lipids 252, 105291.

Salentinig, S., Phan, S., Darwish, T.A., Kirby, N., Boyd, B.J., Gilbert, E.P., 2014. pH-responsive micelles based on caprylic acid. Langmuir 30, 7296-7303.

Sias, B., Ferrato, F., Grandval, P., Lafont, D., Boullanger, P., De Caro, A., Leboeuf, B., Verger, R., Carriere, F., 2004. Human pancreatic lipase-related protein 2 is a galactolipase. Biochemistry 43, 10138-10148.

Small, D.M., Penkett, S.A., Chapman, D., 1969. Studies on simple and mixed bile salt micelles by nuclear magnetic resonance spectroscopy. Biophysica et Biophysica Acta 176, 178-&.

Stejskal, E.O., Tanner, J.E., 1965. Spin Diffusion Measurements: Spin Echoes in the Presence of a Time-Dependent Field Gradient. The Journal of Chemical Physics 42, 288–292.

Timchenko, M., Molchanov, V., Molchanov, M., Timchenko, A., Sogorin, E., 2022. Investigation of lipolytic activity of the red king crab hepatopancreas homogenate by NMR spectroscopy. PeerJ 10, e12742.

Tyl, C., Felsinger, S., Brecker, L., 2004. In situ proton NMR of glycosidase catalyzed hydrolysis and reverse hydrolysis. Journal of Molecular Catalysis B: Enzymatic 28, 55-63.

Vallikivi, I., Järving, I., Pehk, T., Samel, N., Tõugu, V., Parve, O., 2004. NMR monitoring of lipase-catalyzed reactions of prostaglandins: preliminary estimation of reaction velocities. Journal of Molecular Catalysis B: Enzymatic 32, 15–19.

Watanabe, K., Ferrario, M., Klein, M.L., 1988. Molecular dynamics study of a sodium octanoate micelle in aqueous solution. J Phys Chem B 92, 819–821.

Waudby, C.A., Launay, H., Cabrita, L.D., Christodoulou, J., 2013. Protein folding on the ribosome studied using NMR spectroscopy. Prog Nucl Magn Reson Spectrosc 74, 57-75.

Figure legends

Figure 1. *Superimposition of the HSQC [^{1}H, ^{13}C] spectra of MGDG-NaTDC mixed micelles (blue) and NaTDC alone (red).* Mixed micelles of C8-MGDG (50 mM and NaTDC (65 mM) and NaTDC alone (65 mM) were prepared in 500 mM TES buffer, 100 mM NaCl, 5 mM $CaCl_2$, in D_2O, at pD8 and 37 °C. Protons identified as H, H' and H'' correspond to protons of glycerol, acyl chains and galactose, respectively, with their location shown in C8-MGDG structure (insert).

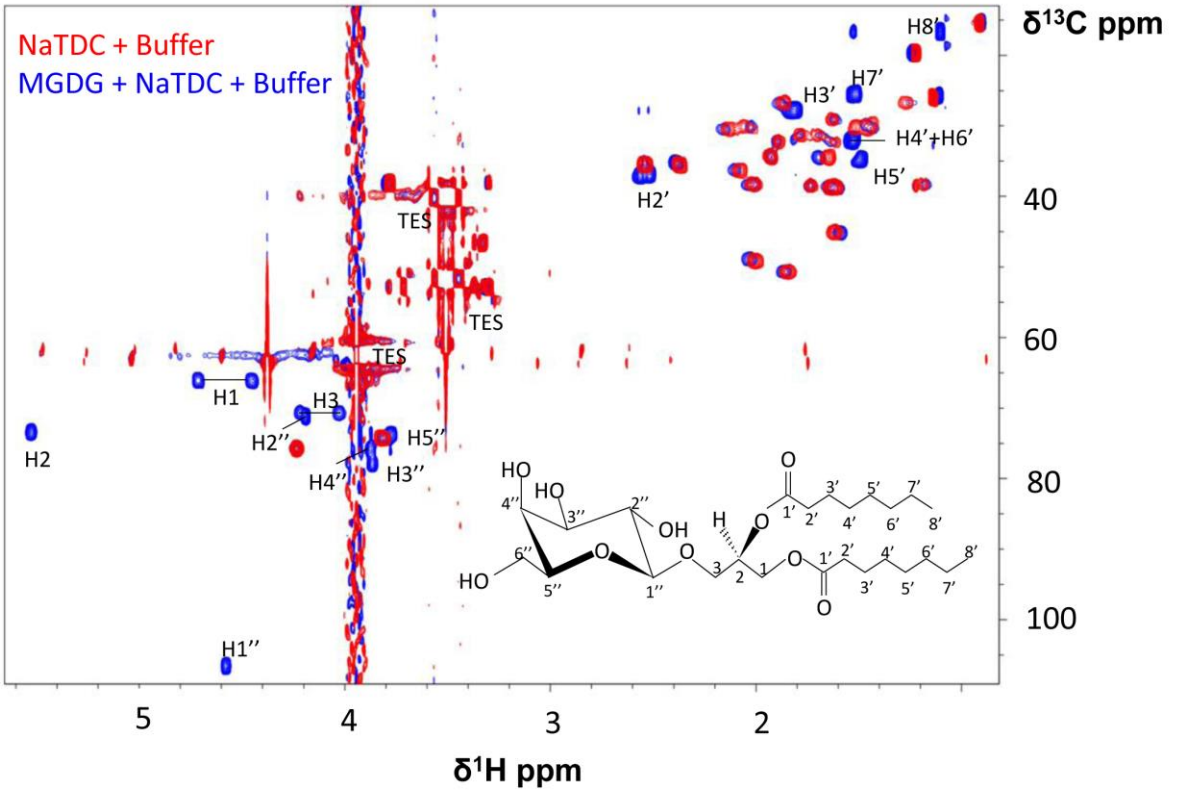

Figure 2. *Superimposition of the HSQC [^{1}H, ^{13}C] spectra recorded in the course of MGDG hydrolysis*. Spectra of the reaction mixture were recorded at the beginning of the reaction (t_0; blue color), during the reaction after the disappearance of MGDG, i.e. after 20 min (black color), and after the completion of the reaction when C8-MGDG was fully converted into MGG and OA (red color). Protons identified as H, H' and H'' correspond to protons of glycerol, acyl chains and galactose, respectively, with their location shown in C8-MGDG structure (insert).

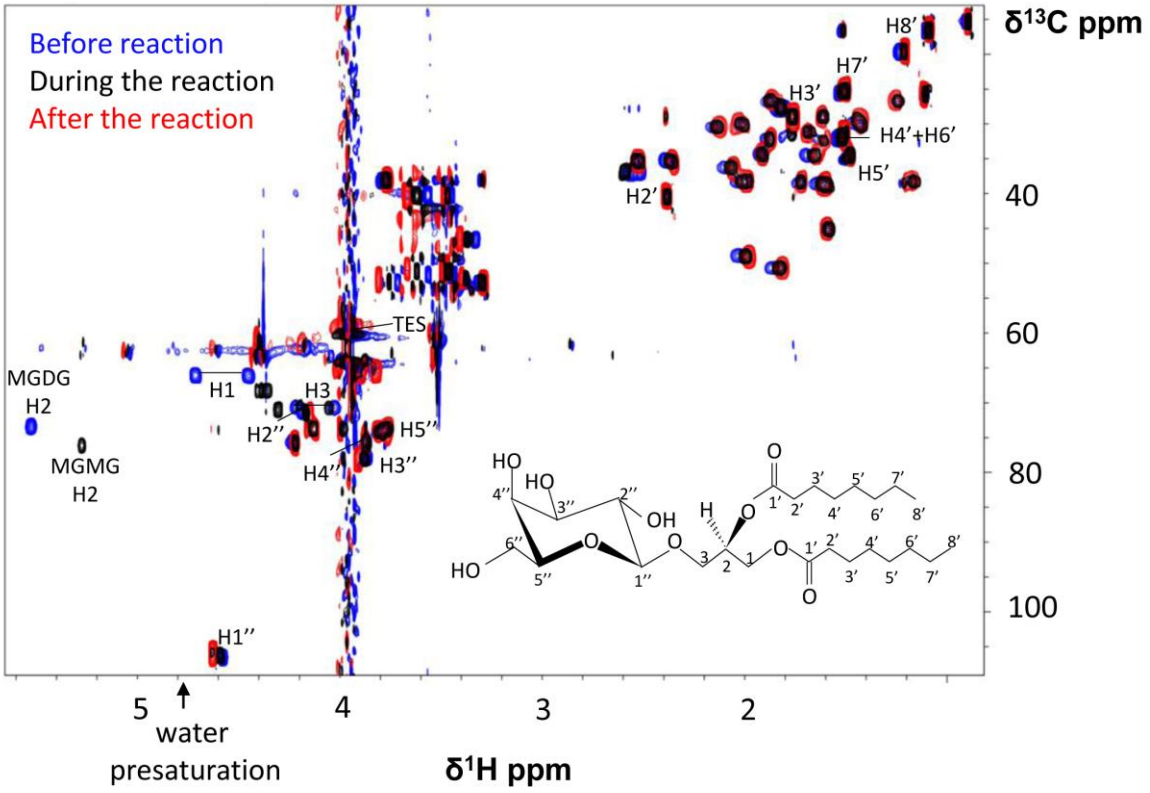

Figure 3. *^{1}H-NMR spectra recorded during the hydrolysis of C8-MGDG-NaTDC mixed micelles by GPLRP2.* Panel A shows the whole ^{1}H-NMR spectrum of C8-MGDG in mixed micelles in which the proton resonances used for quantification (H1, H1", H2 and H2') are indicated. Protons identified as H, H' and H'' correspond to protons of glycerol, acyl chains and galactose, respectively. Panel B shows the time-course evolution of the ^{1}H-NMR spectrum in three specific regions corresponding to H2 (MGDG, MGMG), H1" (MGG, MGMG, MGDG) and H2' (MGMG, MGDG, Free OA). Spectra recorded from times 0 to 17h are shown and superimposed.

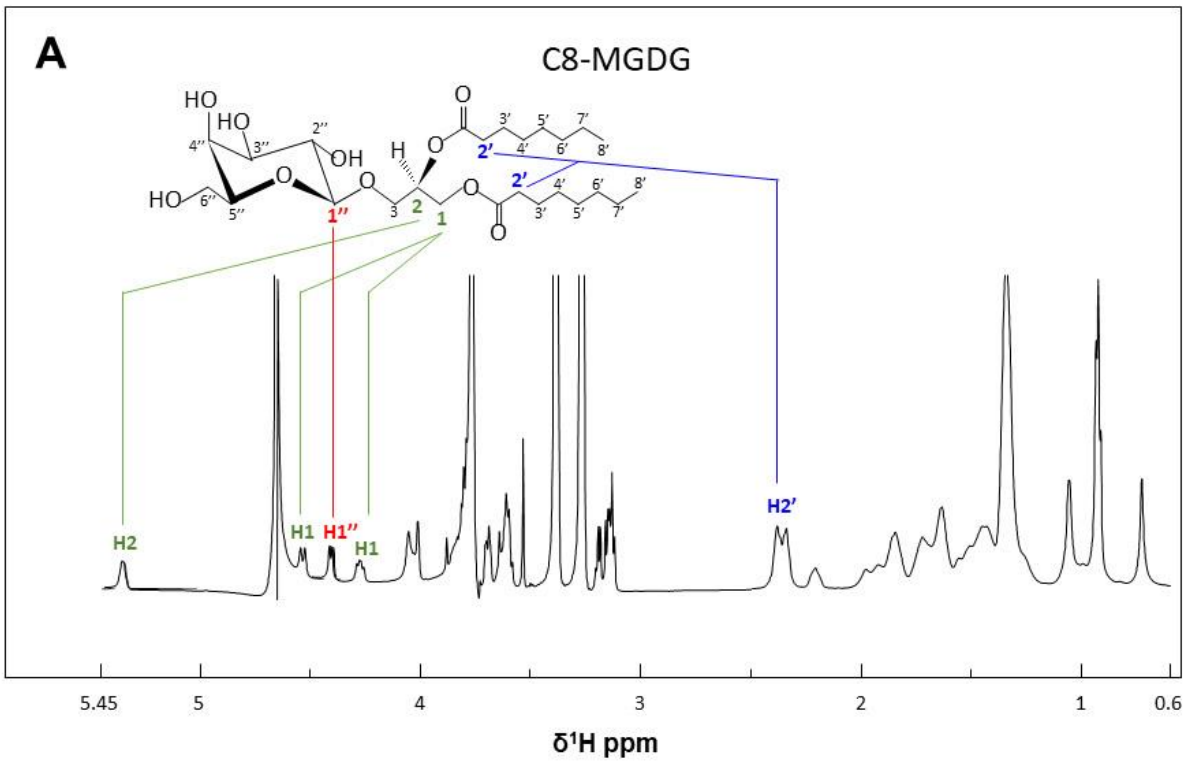

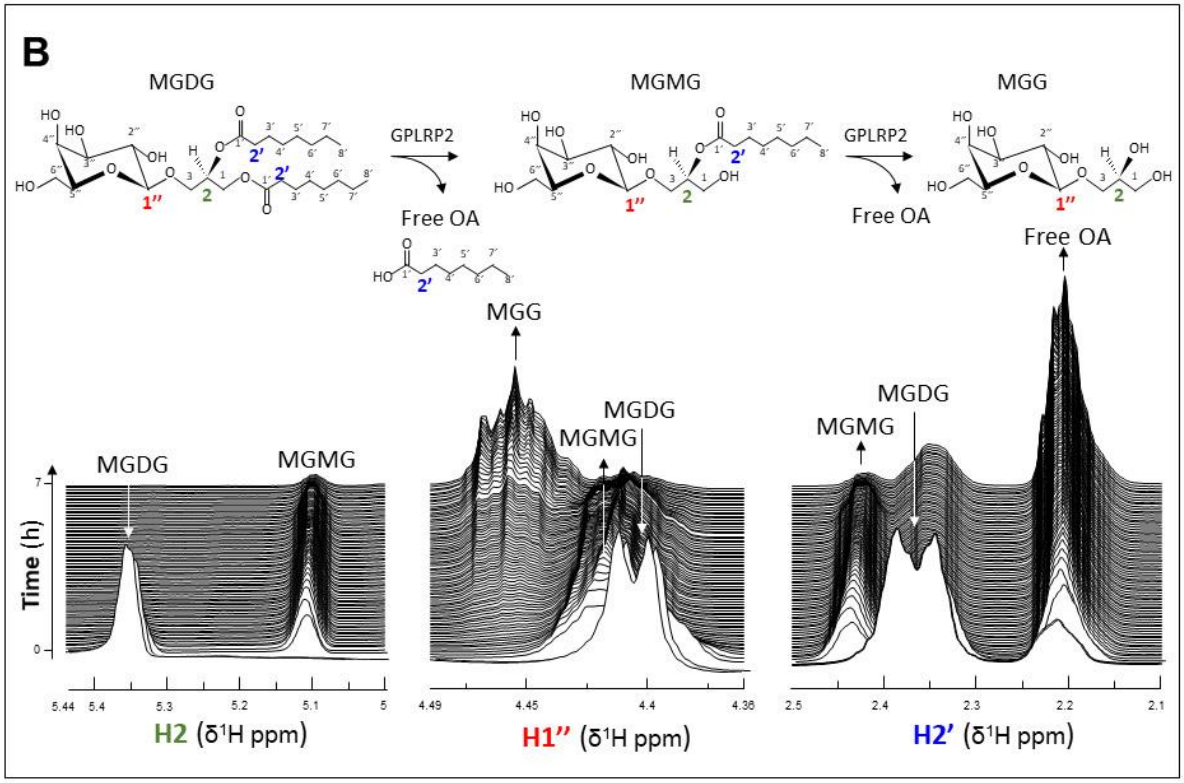
B
MGDG
MGMG
MGG
GPLRP2
GPLRP2
Free OA
Free OA
Free OA
MGG
MGDG
MGMG
MGDG
MGMG
Time (h)
H2 (δ¹H ppm)
H1'' (δ¹H ppm)
H2' (δ¹H ppm)

Figure 4. *Time-dependence of the Pcs of specific MGMG proton resonances*. Pcs were calculated using equation (1).

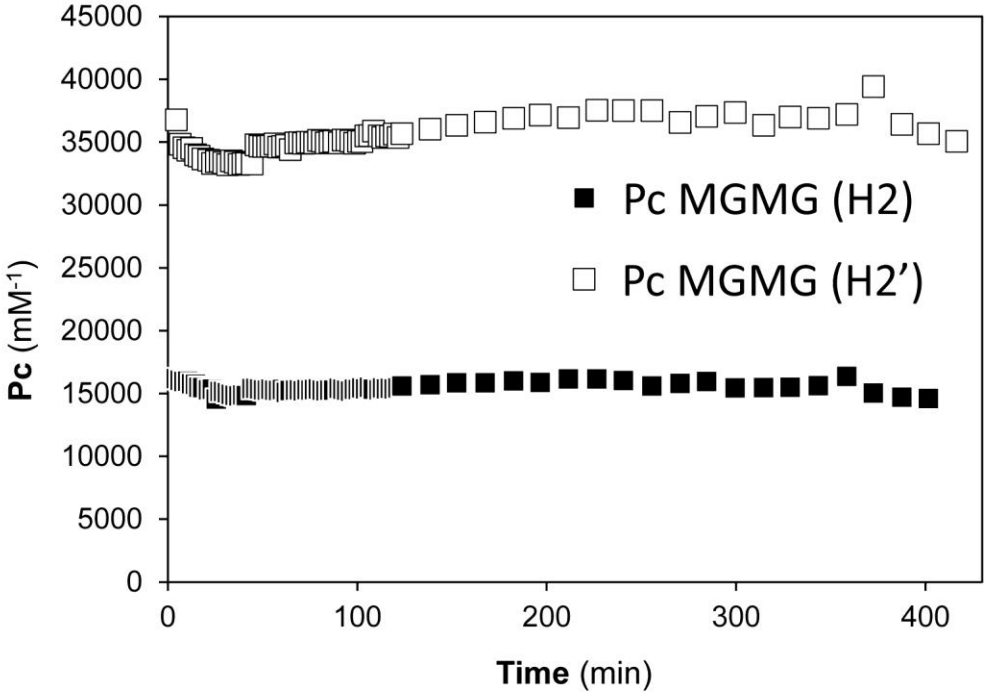

Figure 5. *Time-course variations in C8-MGDG (A) and MGMG (B) concentrations estimated from the resonances of different protons.* Letter a and b corresponds to the two protons H1 bound to glycerol carbon C1 of C8-MGDG (see Table 1).

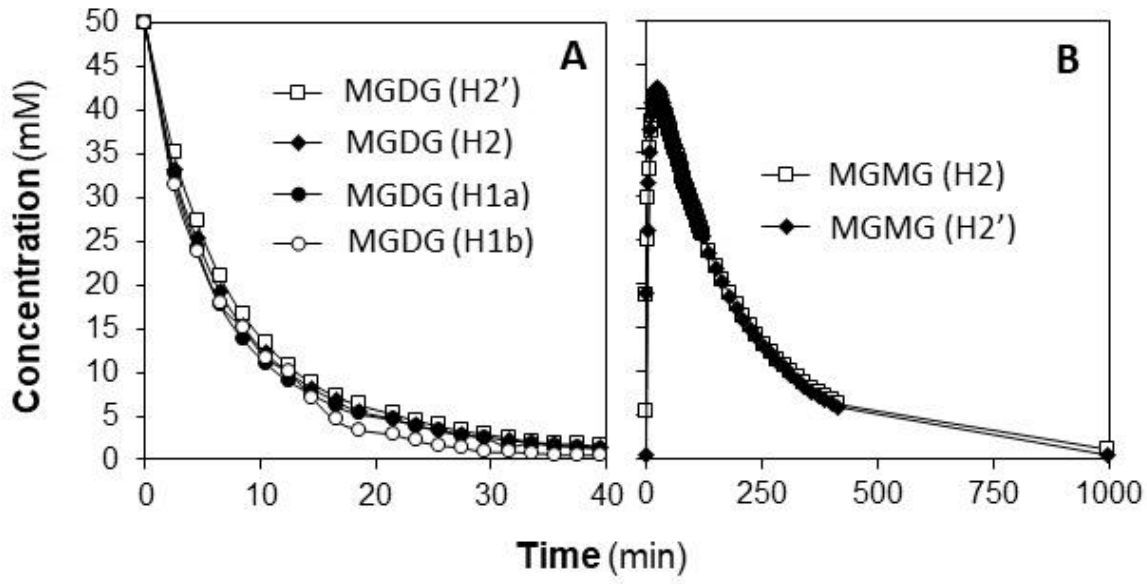

Figure 6. *Time-course variations in the concentrations of lipolysis products and residual substrate during the hydrolysis of C8-MGDG-NaTDC micelles by GPLRP2*. Experiments were monitored using either real-time NMR spectroscopy (Panel A) or TLC-densitometry after lipid extraction (panel B). Hydrolysis of C8-MGDG-NaTDC micelles was catalysed by 100 nM GPLRP2 at pD 8 and 37 °C.

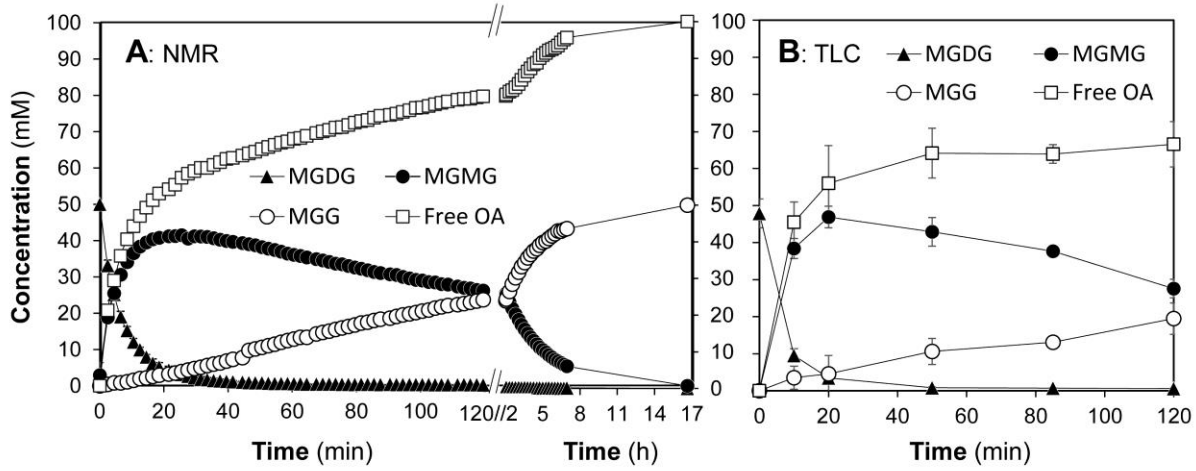

Figure 7. *Mass conservation throughout the lipolysis reaction as estimated from the quantitative analysis of residual C8-MGDG substrate and lipolysis products (MGMG, MGG and free OA) by ^{1}H-NMR spectroscopy.*

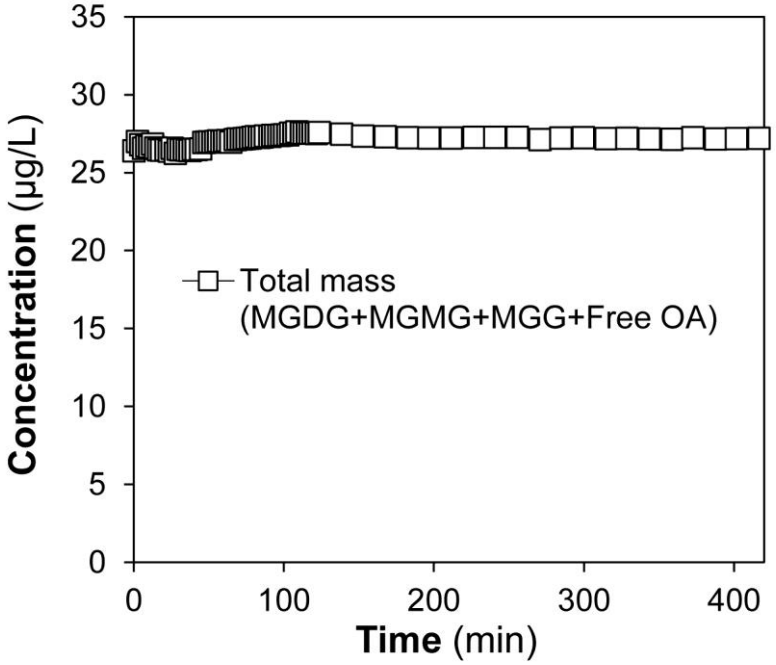

Figure 8. *DOSY-NMR of C8-MGDG substrate, lipolysis products and bile salts in the course of the lipolysis reaction*. Specific resonances of these various compounds led to the determination of their translational diffusion coefficients (D) expressed in $m^2.s^{-1}$ and allowed estimating the hydrodynamic radius (r_H) of the molecular assemblies in which these compounds were present. DOSY spectra recorded on the TES-NaTDC solution (panel A), as well as after addition of MGDG (t=0, panel B), and on the reaction stop at 20 min (panel C) and at the end of the reaction (panel D) are shown. On the top, the ^1H spectra recorded at a low gradient strength is depicted, as well as the resonances chosen to determine the diffusion coefficients. The x-axis of the two-dimensional plots is the proton NMR frequency and the y axis is the diffusion coefficient ($m^2.s^{-1}$) determined using equation (5). A binomial fit was used for the OA resonances. Panels E, F and G show the fit of the diffusion data using equation 5. The x axis is proportional to the square of the gradient strength, with $B = \left[\Delta - \frac{\delta}{3}\right].(\delta.G.\gamma_H)^2$ (refer to the Material and Methods section), and the y axis is $\ln(I/I_0)$. The panel E shows the analysis of the NaTDC resonances in TES (black), at t=0 (blue), at t=20 min (red) and at the end of the reaction (green). The panel F shows the glycerol H2 and acyl H2' resonances of MGDG at t=0 (blue) and at time t=20min (red), and of MGMG at t=20min (black), as well as the galactose resonances of MGG at the end of the reaction. The panel G shows the OA acyl resonances at t=20min (red) and at the end of the reaction (green).

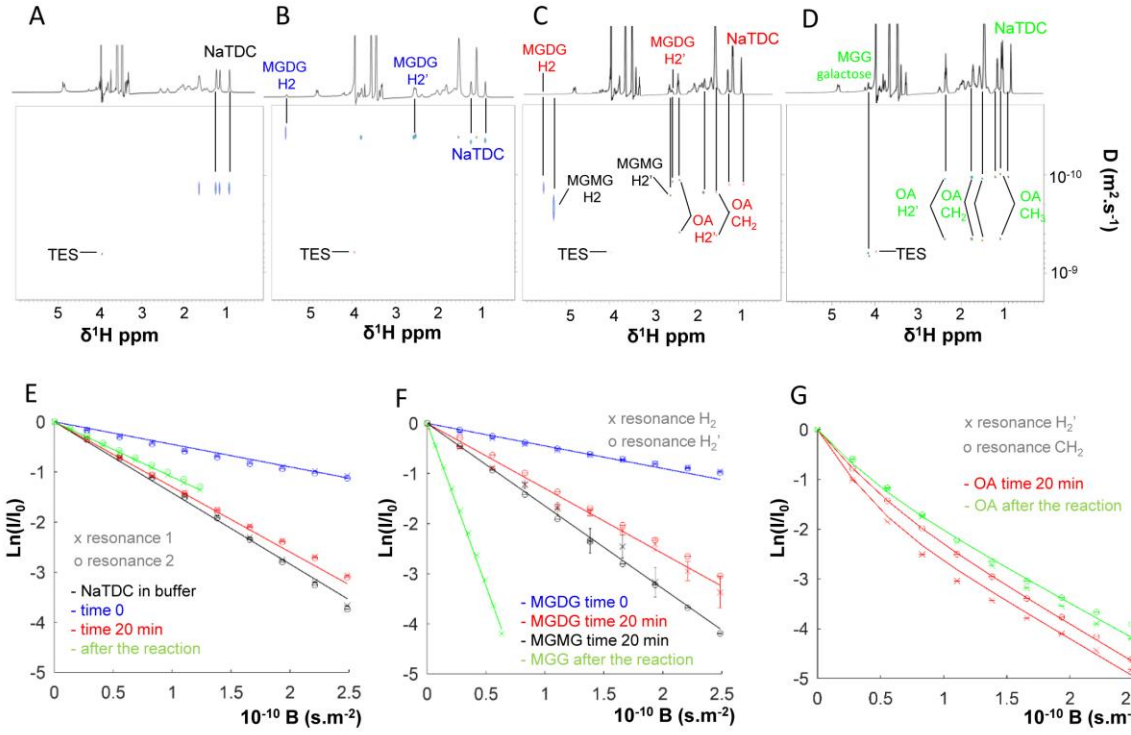
A
B
C
D
NaTDC
MGDG H2
MGDG H2'
MGMG H2
MGMG H2'
OA H2'
OA CH2
MGG galactose
OA CH3
TES
δ¹H ppm
D (m².s⁻¹)
10⁻¹⁰
10⁻⁹
E
F
G
Ln(I/I0)
x resonance 1
o resonance 2
- NaTDC in buffer
- time 0
- time 20 min
- after the reaction
x resonance H2
o resonance H2'
- MGDG time 0
- MGDG time 20 min
- MGMG time 20 min
- MGG after the reaction
x resonance H2'
o resonance CH2
- OA time 20 min
- OA after the reaction
10⁻¹⁰ B (s.m⁻²)

Figure 9. *Schematic representation of changes in lipid composition and colloidal structures upon the hydrolysis of MGDG by GPLRP2*. The sizes (hydrodynamic radius (r_H)) of the molecular aggregates (micelles) formed by MGDG, MGMG, bile salts (NaTDC) and OA in the course of the lipolysis reaction were deduced from DOSY-NMR spectroscopy experiments.

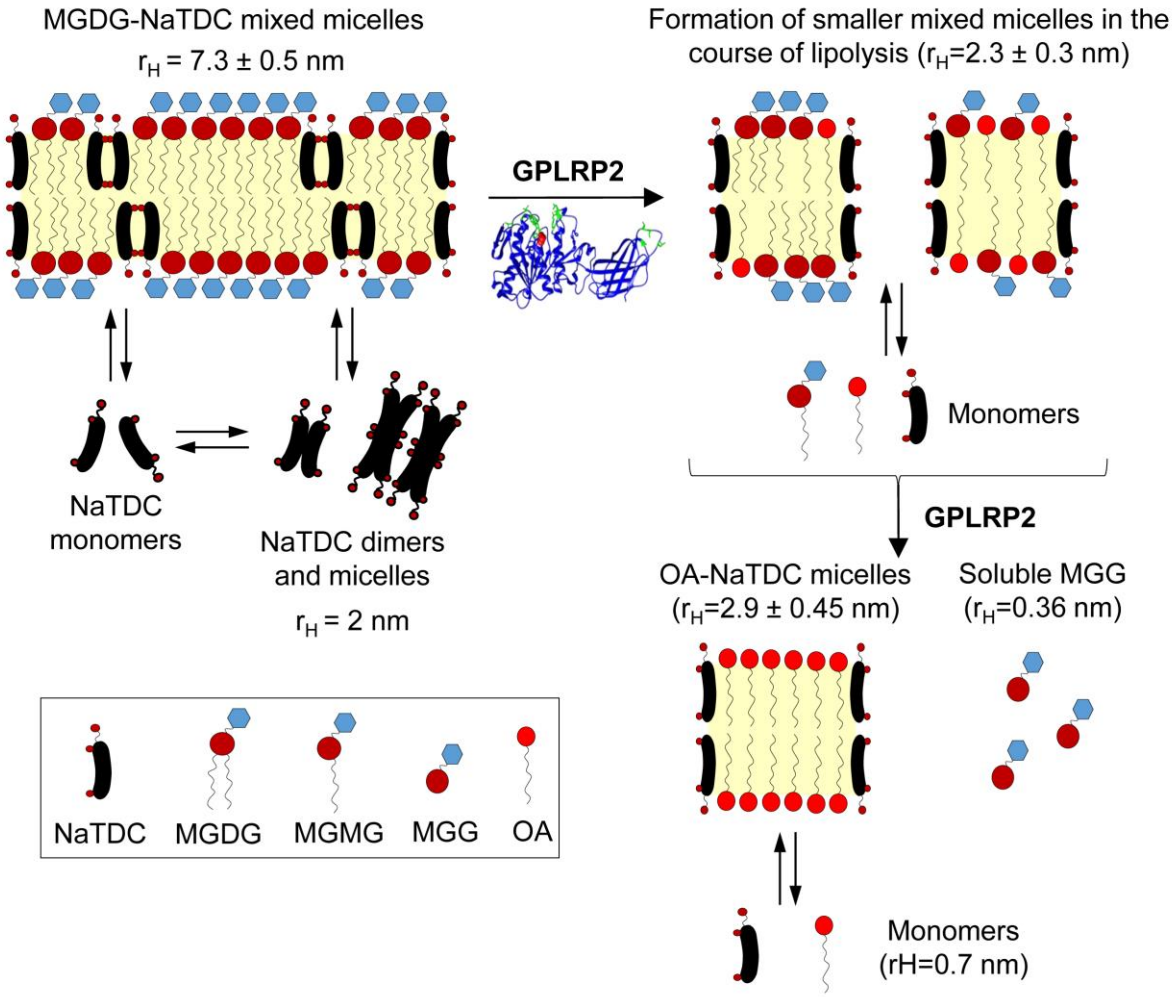

Table 1: ^{1}H and ^{13}C NMR chemical shifts of C8-MGDG, C8-MGMG, MGG and free OA.

Compound	Proton	^{1}H (ppm)				Carbone	^{13}C (ppm)			
		MGDG	MGMG	MGG	Free OA		MGDG	MGMG	MGG	Free OA
Glycerol	H1	4.12 3.93	4.05 3.91	4.07 3.92		C1	70.5	73.6	73.4	
	H2	5.43	5.19	-		C2	73.2	76.2	-	
	H3	4.62 4.35	4.31 4.27	-		C3	66.0	68.1	-	
OA	H8’	1.00	1.00		1.00	C8’	16.7	16.7		16.7
	H7’	1.42	1.42		1.42	C7’	25.5	25.5		25.5
	H6’	1.42	1.42		1.42	C6’	32.1	32.1		32.1
	H5’	1.40	1.40		1.40	C5’	34.6	34.6		34.6
	H4’	1.42	1.42		1.42	C4’	32.1	32.1		32.1
	H3’	1.71	1.74		1.68	C3’	27.8	27.5		28.8
	H2’	2.46 2.42	2.51		2.30	C2’	37.0 36.9	36.7		40.4
Galactose	H1”	4.48	4.51	4.55		C1”	106.5	106.4	106.0	
	H2”	3.67	3.69	3.69		C2”	73.5	73.7	73.7	
	H3”	3.77	3.78	3.79		C3”	75.6	75.5	75.5	
	H4”	4.09	4.08	4.07		C4”	71.1	71.2	71.3	
	H5”	3.77	3.79	3.83		C5”	77.7	77.9	77.9	
	H6”	(a) -	-	-		C6”	-	-	-	

Table 2: *Proportionality coefficients (Pc) of C8-MGDG, MGG and Free OA protons obtained using their initial and final concentrations, respectively.*

$Pc^{H_2}_{MGDG}(t_0)$	$Pc^{H''_6(a)}_{MGDG}(t_0)$	$Pc^{H''_6(b)}_{MGDG}(t_0)$	$Pc^{H'_2}_{MGDG}(t_0)$	$Pc^{H''_1}_{MGG}(t_f)$	$Pc^{H'_2}_{Free\ OA}(t_f)$
17242 mM^{-1}	12917 mM^{-1}	14222 mM^{-1}	60678 mM^{-1}	13703 mM^{-1}	32804 mM^{-1}

***Table 3**: Diffusion coefficients (D, $m^2.s^{-1}$) and hydrodynamic radii (r_H, nm) of the main aggregates containing NaTDC, MGDG and lipolysis products at different stage of the reaction.*

Hydrodynamic radii of the aggregates were estimated using the resonances assigned to H2 and H2" protons of C8-MGDG, H2 and H2" proton from MGMG, H2 and galactose protons from MGG and H2' and CH_2 protons from OA. A binomial fit was used for the OA resonance, and an approximation of their relative signal intensities are indicated in brackets. This is not directly related to the relative population because signal intensity is also function of the size of the particle and the tumbling time of the molecules.

Compound	*Condition and time*	*D ($m^2.s^{-1}$)*	*r_H (nm)*
NaTDC	Alone in buffer	$1.4 \pm 0.1\ 10^{-10}$	2.3 ± 0.2
	Initial mixed micelles	$4.5 \pm 0.5\ 10^{-11}$	7.3 ± 0.5
	During the reaction	$1.3 \pm 0.2\ 10^{-10}$	2.3 ± 0.3
	End of the reaction	$1.1 \pm 0.2\ 10^{-10}$	2.9 ± 0.4
C8-MGDG	Initial mixed micelles	$4.5 \pm 0.5\ 10^{-11}$	7.3 ± 0.5
	During the reaction	$1.3 \pm 0.2\ 10^{-10}$	2.3 ± 0.3
MGMG	During the reaction	$1.65 \pm 0.15\ 10^{-10}$	2 ± 0.5
OA	During the reaction	$4.5 \pm 0.5\ 10^{-10}$ (60-70%) $1.5 \pm 0.2\ 10^{-10}$ (30-40%)	0.7 ± 0.1 (60-70%) 2.2 ± 0.4 (30-40%)
	End of the reaction	$4.6 \pm 0.5\ 10^{-10}$ (95%) $1.1 \pm 0.2\ 10^{-10}$ (5%)	0.7 ± 0.1 (95%) 2.9 ± 0.5 (5%)
MGG	End of the reaction	$6.5 \pm 1\ 10^{-10}$	0.5 ± 0.1